Funded by EU's Horizon 2020

D 6.5

CARDIO-VASCULAR DEVICE TESTING REPORT

DISCLAIMER

AKNOWLEDGEMENT

This project has received funding from the European Union's Horizon 2020 research and innovation programme under grant agreement No.769661.

This project has received funding from the European Union's Horizon 2020
research and innovation programme under grant agreement No 769661

Supporting Active Ageing through Multimodal coaching

DELIVERABLE DOCUMENTATION SHEET

Deliverable:	D6.5 Cardio-Vascular Device Testing Report
WP №	6
Title:	Specialised Well-Being Monitoring and Assessment
Editor(s):	Aleksandra Rashkovska Koceva
Contributor(s):	Roman Trobec, Viktor Avbelj, Matjaž Depolli, Miha Mohorčič
Type:	Report
Version:	v1.0
Submission Due Date:	30.09.2019
Dissemination level (CO/PU):	CO
Copyright:	©SAAM Project - All rights reserved

☒ Approved by the WP Leader

☒ Approved by the Technical/Exploitation Manager[1]

☒ Approved by the Coordinator

☒ Approved by the PSC

[1] Choose Technical Manager for Deliverables in WP1-7,10 and Exploitation Manager in WP 8-10

This project has received funding from the European Union's Horizon 2020 research and innovation programme under grant agreement No 769661

PUBLISHABLE SUMMARY

In this report, we present the work performed in the scope of T6.5: Cardio-Vascular Health Monitoring. The cardio-vascular module in SAAM covers two main functionalities: monitoring of the heart rhythm and monitoring of the blood pressure. The Savvy ECG sensor is used for heart rhythm monitoring, i.e. for electrocardiogram (ECG) monitoring. The Sanitas SBM 67 was selected as a blood pressure monitor demo device for the project. The work performed in the scope of this task is divided in two groups: (i) research related activities and (ii) SAAM integration activities. The research work concerns ECG acquisition and analysis in relation to the SAAM project. We address two challenges for patch ECG signal analysis: heartbeat detection and heartbeat classification. Furthermore, we have tested the option to enrich the ECG with activity data. The purpose of these studies was to explore the feasibility for their inclusion into the SAAM system. At the end of this report, we describe the integration of the cardio-vascular module in the SAAM infrastructure, i.e. the protocols for transfer of ECG measurements from the Savvy sensor and the blood pressure measurements into the SAAM system. These activities are in relation to T2.3: User-Sided IT Infrastructure. Furthermore, for providing relevant heart-related features for the tasks concerned with modelling, profiling and coaching in WP4, we present the implementation of a real-time ECG feature extraction. Lastly, we describe the testing scenarios in which the cardio-vascular module can be used in SAAM pilots in WP8.

This project has received funding from the European Union's Horizon 2020
research and innovation programme under grant agreement No 769661

QUALITY CONTROL ASSESSMENT SHEET

Version	Date	Comment	Name of author/reviewer/contributor
V0.1	06.09.2019	First Draft	Aleksandra Rashkovska Koceva
	09.09.2019	Review First Draft	Matjaž Depolli, Roman Trobec, Viktor Avbelj
	10.09.2019	Contributions	Miha Mohorčič
V0.2	12.09.2019	Second Draft	Aleksandra Rashkovska Koceva
	18.09.2019	1st Peer review[2]	Saturnino Luz (UEDIN), Fasih Haider (UEDIN)
	23.09.2019	2nd Peer review	Mihael Mohorčič (JSI)
V1.0	24.09.2019	Final Draft	
	24.09.2019	WP Leader approval	
	25.09.2019	Coordinator approval	
		EAB Review	N.a.
	30.09.2019	PSC approval	
V1.0	01.10.2019	Submission to EC	

HISTORY OF CHANGES

For updating the Deliverable after submission to the EC if applicable

Version	Date	Change
V2.0		

[2] Each Deliverable to have two experts (partners) assigned for Peer review. The experts should be different from the Experts, contributing to its creation. List of Deliverables and Peer review experts to be decided at Kick-off.

This project has received funding from the European Union's Horizon 2020 research and innovation programme under grant agreement No 769661

Supporting Active Ageing through Multimodal coaching

PROJECT DOCUMENTATION SHEET

Project Acronym:	SAAM
Project Full Title:	Supporting Active Ageing through Multimodal coaching
Grant Agreement:	GA № 769661
Call identifier:	H2020-SC1-2017-CNECT-1
Topic:	Personalised coaching for well-being and care of people as they age
Action:	Research and Innovation Action
Project Duration:	36 months (1 October 2017 – 30 September 2020)
Project Officer:	Jose Albacete VALVERDE
Coordinator:	Balkan Institute for Labour and Social Policy (BILSP)
Consortium partners:	Jožef Stefan Institute (JSI) University of Edinburgh (UEDIN) Paris-Lodron Universität Salzburg (PLUS) Scale Focus AD (SCALE) Interactive Wear AG (IAW) Univerzitetni rehabilitacijski inštitut Republike Slovenije (SOČA) Nacionalna Katolicheska Federacia CARITAS Bulgaria (CARITAS) Bulgarian Red Cross (BRC) Eurag Osterreich (EURAG)
website:	saam2020.eu
social media:	#saam2020, #saamproject

This project has received funding from the European Union's Horizon 2020 research and innovation programme under grant agreement No 769661

ABBREVIATIONS

AAMI	Association for the Advancement of Medical Instrumentation
BLE	Bluetooth Low Energy
BPM	Blood pressure monitor
ECG	Electrocardiogram
EMA	Exponential moving-average
GW	Gateway
HCTSA	Highly Comparative Time Series Analysis
HR	Heart rate
MEMS	Micro Electro Mechanical System
SAAM	Supporting Active Ageing through Multimodal Coaching
PPT	Personal portable terminal
WHO	World Health Organization

This project has received funding from the European Union's Horizon 2020
research and innovation programme under grant agreement No 769661

CONTENTS

This project has received funding from the European Union's Horizon 2020 research and innovation programme under grant agreement No 769661

TABLE OF FIGURES

This project has received funding from the European Union's Horizon 2020 research and innovation programme under grant agreement No 769661

This project has received funding from the European Union's Horizon 2020 research and innovation programme under grant agreement No 769661

1. INTRODUCTION

The cardio-vascular module in SAAM covers two main functionalities: monitoring of the heart rhythm and monitoring of the blood pressure. The **Savvy ECG** sensor (http://www.savvy.si/en/) is used for heart rhythm monitoring, i.e. for electrocardiogram (ECG) monitoring. The **Sanitas SBM 67** blood pressure monitor (BPM) with Bluetooth Low Energy (BLE) connecting capabilities was selected as a blood pressure monitor demo device for the project. The readings from the BPM will be used in SAAM as the device provides them. Providing the BPM readings in the SAAM system, i.e. connecting the BPM in the SAAM infrastructure is the main activity concerning blood pressure monitoring. However, the acquisition and analysis of the ECG for the purpose of the SAAM project requires more attention and therefore, this deliverable concerns these activities in more details. Namely, ECG signals obtained from patch ECG sensors, like Savvy ECG, in normal daily activities, are more challenging from the signal processing perspective, since they are more contaminated with noise and artefacts, compared to the ECGs obtained in clinical settings. This makes detection of prominent signal features, like R-peaks, and the calculation of the heart rate, much more challenging compared to the standard clinical settings. In the latter, subjects are supposed to be lying down and be relaxed, not to cause skeletal muscle electrical activity, which may be picked up with the same electrodes measuring the ECG.

In this report, we present the work performed in the scope of T6.5: Cardio-Vascular Health Monitoring, which can be divided in two groups: research related activities and SAAM integration activities. We begin this deliverable with Section II by describing the used cardio-vascular devices, i.e. the Savvy ECG and the BPM. Sections III, IV and V present the research work conducted on ECG acquisition and analysis in relation to the SAAM project. We address two challenges for patch ECG signal analysis: heartbeat detection [1] and heartbeat classification [2]. In Sections III and IV, for these activities, we describe the problem, including related work, describe the investigated methods, and present and discuss the results. Furthermore, we have tested the option to enrich the ECG with activity data [3]. For that activity, in Section V, we present the procedure for measurements and the preformed analysis.

The results from all these research activities are important for the implementation of the cardio-vascular module in the SAAM system. The aim of these studies is to explore the feasibility for their inclusion into the SAAM system. For that purpose, we describe, in Section VI, the integration of the cardio-vascular module in the SAAM infrastructure and the relation of the Task T6.5 to other WPs/Tasks. Namely, we describe the protocols for transfer of ECG measurements from the Savvy sensor and the blood pressure measurements from the BPM into the SAAM system, i.e. to the Edge Gateway (GW). These activities are in relation to the Task T2.3: User-Sided IT Infrastructure. Furthermore, for providing relevant heart-

This project has received funding from the European Union's Horizon 2020 research and innovation programme under grant agreement No 769661

related features for the Tasks concerned with modelling, profiling and coaching in WP4, we present the implementation of a real-time ECG feature extraction on the Edge GW. Lastly, we present the envisioned testing scenarios for using the cardio-vascular module in the SAAM pilots in WP8. The cardio-vascular pilot methodology and accompanying data collection instruments are part of WP8 documentation.

2. CARDIO-VASCULAR DEVICES

The wireless ECG body sensor was originally developed by JSI before the SAAM project commenced. The know-how was transferred for final design and production by Saving d.o.o., Slovenia under the commercial name "Savvy". Savvy ECG is graded as a medical device with CE certificate, dimensions of 10 cm and weight of 21 g, including a small battery, BLE radio and a low-power signal processor. Its analogue part is designed in a way that it is able to capture significantly smaller signals than in standard ECGs because of a smaller distance between the differential electrodes. A 10-bits A/D converter is used and sample rates of up to 512 samples/s can be set. The measured ECG is wirelessly transmitted to a personal terminal, e.g. a Smartphone, where it is saved in a file. The design of the Savvy sensor hardware and firmware is a compromise between technical performances and extremely low power consumption. The ECG sensor is non-obtrusive with a complete autonomy of 7 days of continuous measurement, which makes it ideal for long-term heart rhythm monitoring. Besides ECG, other features can be extracted from the measured potential, e.g., muscle activity and respiration [4]. The Savvy ECG has already been described as a part of the system infrastructure in D1.8: System technical specification.

Figure 1: Savvy ECG placed on the charger.

This project has received funding from the European Union's Horizon 2020
research and innovation programme under grant agreement No 769661

Sanitas SBM 67 BPM is an upper arm BPM used to carry out non-invasive measurement and monitoring of the arterial blood pressure values in adults. It allows quick and easy measurement of the blood pressure, saving the measured values and displaying the average values of the measured values taken. The recorded values are classified according to the World Health Organization (WHO) guidelines. It is also possible to transfer the measured values saved on the device using Bluetooth® Smart.

Figure 2: Sanitas SBM 67 blood pressure monitor.

3. HEARTBEAT DETECTION

3.1. Background and Objectives

Heartbeat detection is an initial and fundamental step for ECG analysis, segmentation, clustering [5] and classification. It is the detection of the times when heartbeats occur, which is essentially the detection of the times of the R-peaks. Accurately determined R-peaks are necessary also for validation of R-R [6] or Q-T [7] variability, and detailed analysis of P-waves [8]. Specialized heartbeat detectors are needed for the extraction of fetal ECG [9]. Finally, reliable and robust heartbeat detectors are essential in the monitoring and diagnostics of irregular rhythm and arrhythmias [10].

There are many different approaches to heartbeat detection published in literature [11], some of which are specifically targeting mobile ECG devices [12]. These algorithms have not yet been tested on the measurements obtained directly with patch ECG devices, which are becoming more popular by the day, since they are easy to use and wireless [13]. We have tested functions for heartbeat detection from the "WFDB Toolbox for MATLAB and Octave" [14, 15] and "Cardiovascular Signal Toolbox" [16], both from the PhysioNet[3], which is a free collection of recorded physiologic signals and related open-source software. We have also applied a simple wavelet-based heartbeat detection algorithm, to have one

[3] https://physionet.org/

This project has received funding from the European Union's Horizon 2020
research and innovation programme under grant agreement No 769661

algorithm outside of the PhysioNet to compare with. For calculating the heart rate, the number of detected heartbeats is the most relevant. Therefore, our purpose was to examine if the algorithms detect the correct number of heartbeats.

3.2. Material and Methods

We have conducted a research study where we recorded two ECGs from each of the ten study participants (age range 25-63 years, 9 males, 1 female): one ECG in a sitting position and one while running on a treadmill. Each measurement lasted from 30 s to 1 min. While in sitting position, the subjects were asked to be completely relaxed. The measurements were obtained with the Savvy patch ECG [17], which was positioned according to Fig. 3. The subjects were asked to put one of the electrodes at the end of the sternum bone, and the other horizontally to the right, and to press the self-adhesive electrodes to the skin to achieve a proper contact. The subjects did not shave and did not apply any special cleaning of the skin before usage. The sampling frequency was 128 Hz. Informed consent for using the acquired measurements in a research study was obtained from all participant and data was de-personalized before further analysis.

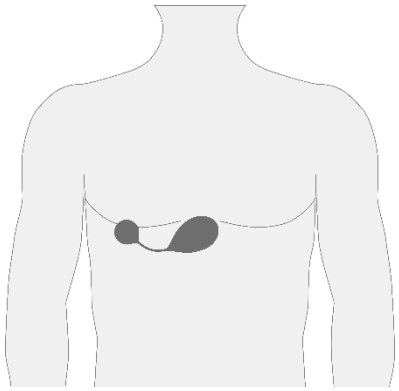

Figure 3: Positioning of the Savvy patch ECG.

The PhysioNet Cardiovascular Signal Toolbox is an open-source modular program implemented in MATLAB mainly for the purpose to calculate heart rate variability. We have used the following functions: *jqrs*, *run_sqrs* and *wqrsm*. The *jqrs* [18, 19] is an implementation of the Pan- Tompkins [20] algorithm that finds R-peaks, while *run_sqrs* and *wqrsm* (detect Q-waves) are re-programmed original *sqrs* and *wqrs* functions from the Physionet WFDB library. The WFDB Toolbox for MATLAB and Octave is a set of

This project has received funding from the European Union's Horizon 2020 research and innovation programme under grant agreement No 769661

wrapper functions for the PhysioNet's WFDB Software Package and other PhysioToolkit applications. We have tested the following functions: *ecgpuwave*, *gqrs*, *sqrs*, and *wqrs* [21]. The *ecgpuwave* is based on the Pan-Tompkins algorithm and returns a number of fiducial points on the ECG (we used only R-peaks). The other three functions return the locations of the Q-wave. All four functions are wrappers for the WFDB library functions with the corresponding names. The *wavelet* algorithm was adopted from the MATLAB documentation [22].

The data was imported in MATLAB and processed with the heartbeat detection functions. We did not filter the data before applying the functions, since the required filtering is implemented within the functions. All raw measurements were examined by two independent observers who identified the correct locations of R-peaks. Each measurement was then plotted with correct R-peaks and the QRS location information obtained from each of the heartbeat detection algorithms (see Fig. 4). The observers independently marked the heartbeats that were not recognized (false negatives - FN) and the falsely identified heartbeats (false positives - FP). A plot showing two ECG segments with correct R-peaks and those identified by the *sqrs* algorithm is shown in Fig. 4. The star before the third heartbeat is an example of fiducial point (in this case Q-wave) detected at a wrong location. We have however considered this and similar situations as correct heartbeat identification, because the time shift in the detection of a particular fiducial point does not significantly affect the heart rate calculation. From the number of FPs and FNs we have calculated the relative numbers (RFP and RFN respectively) by dividing them with the total number of peaks in each measurement, to accommodate for the different measurement lengths and different heart rates between subjects.

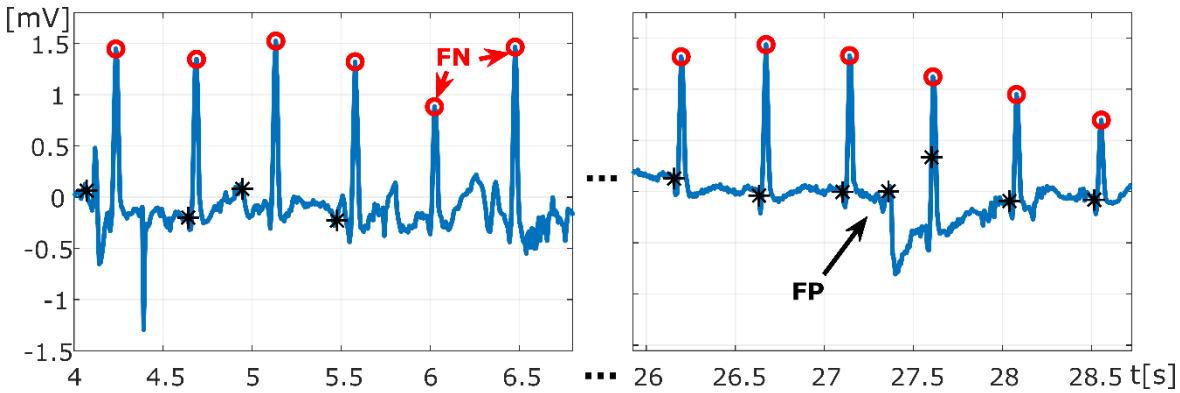

Figure 4: Two excerpts from a treadmill measurement containing two FNs (left figure) and one FP (right figure). Red circles are the correct locations of the R-peaks, whereas the black asterisks are the Q-wave locations determined by the sqrs function from the Cardiovascular Signal Toolbox.

This project has received funding from the European Union's Horizon 2020
research and innovation programme under grant agreement No 769661

3.3. Results and Discussion

The agreement between the two observers was 100%. The absolute numbers of FPs and FNs for each method and for each measurement are given in Table 1. The obtained relative numbers of FPs and FNs is shown in Fig. 5. Table 2 shows the percentage of FN and FP heartbeat detections for each measurement and for the two different setting: sitting and running. From Fig. 5, it is obvious that the *ecgpuwave* and the *gqrs* methods from the WFDB toolbox have very low relative number of FNs and FPs, but most of the functions showed very high performance in detecting heartbeats. The only exceptions are *run_sqrs* and *sqrs* from the Cardiovascular Signal Toolbox, which had problems in finding heartbeats in very noisy measurements, and the *wavelet* approach, which had a lot of both FPs and FNs. This is visible in more detail in Table 2.

Table 1: Number of false negatives (FN) and false positives (FP) heartbeats for each method and for each measurement.

Measurement number:		**1**	**2**	**3**	**4**	**5**	**6**	**7**	**8**	**9**	**10**	**11**	**12**	**13**	**14**	**15**	**16**	**17**	**18**	**19**	**20**
Methods																					
jqrs	**FN**	0	4	0	0	3	0	0	15	0	2	0	0	0	0	0	0	0	11	1	0
	FP	0	0	0	0	0	0	0	0	0	0	0	0	0	0	0	0	0	0	0	0
run_sqrs	**FN**	0	44	0	63	0	38	0	61	1	3	0	17	0	15	0	36	0	13	1	1
	FP	0	4	25	0	0	0	0	0	0	1	0	3	0	2	0	0	0	11	0	27
wqrsm	**FN**	0	0	0	0	0	0	0	0	0	0	0	0	0	0	0	0	0	0	0	0
	FP	0	44	0	2	0	20	0	16	0	1	0	7	0	0	0	14	0	28	0	0
ecgouwave	**FN**	1	3	1	1	1	1	1	17	0	1	1	1	0	0	1	1	1	0	0	0
	FP	0	11	0	0	0	0	0	0	0	0	0	0	0	0	0	5	0	1	0	0
gqrs	**FN**	0	0	0	0	0	0	0	0	0	1	0	0	0	1	3	6	0	0	0	0
	FP	0	17	0	1	0	0	0	5	0	1	0	15	0	0	0	1	0	11	0	0
sqrs	**FN**	1	6	0	0	0	1	0	38	1	0	0	0	0	0	1	42	0	3	0	0
	FP	0	4	0	0	0	1	0	0	0	0	0	3	0	1	0	0	0	1	0	0
wqrs	**FN**	0	0	0	0	0	0	0	0	0	0	0	0	0	0	0	0	0	0	0	0
	FP	0	29	0	0	0	2	0	6	0	0	0	2	0	0	0	11	0	15	0	0
wavelet	**FN**	0	0	0	0	0	0	0	0	0	0	0	0	0	0	30	33	29	2	0	0
	FP	0	46	38	29	0	33	0	33	0	2	0	21	0	27	0	0	0	26	0	35
Total number of heartbeats		46	76	38	70	65	73	46	81	72	65	31	56	40	54	40	47	28	57	34	50

This project has received funding from the European Union's Horizon 2020 research and innovation programme under grant agreement No 769661

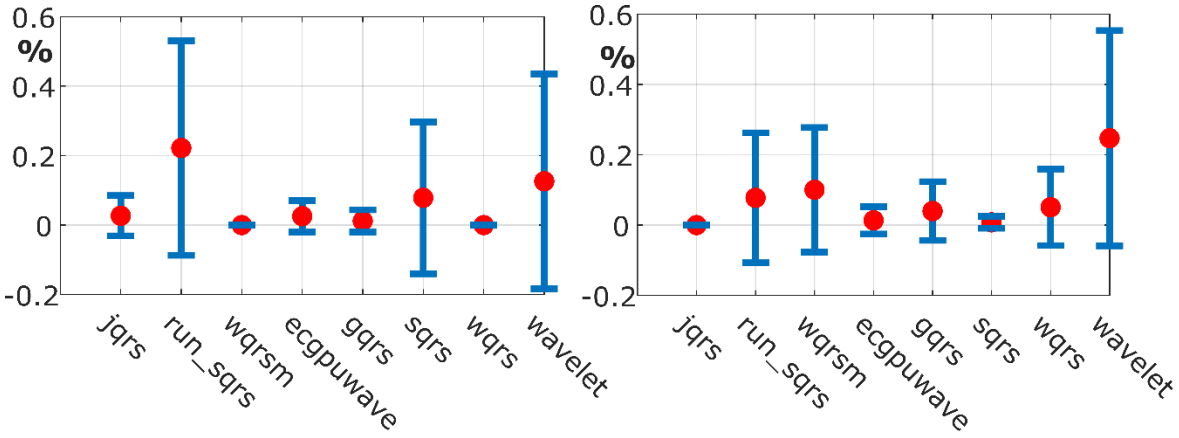

Figure 5: Left: Mean and standard deviation of the relative number of FNs. Right: Mean and standard deviation of the relative number of FPs. The relative number of FNs and FPs was calculated by dividing the number of missed heartbeats and falsely identified heartbeats (respectively) with the total number of heartbeats in each measurement.

Table 2: Percentage of FP and FN heartbeats for each method while sitting, while running, and in total (FP and FN together).

	Sitting		Running		Total
Method	**FN**	**FP**	**FN**	**FP**	
jqrs	0.9	0	5.1	0	**1.7**
run_sqrs	0.5	**5.7**	**46.3**	7.6	17.1
wqrsm	0	0	0	**21**	6.2
ecgpuwave	**1.6**	0	4.0	2.7	**2.3**
gqrs	0.7	0	1.3	8.1	**2.9**
sqrs	0.7	0	**14.3**	1.6	4.8
wqrs	0.0	0	0	10.3	**3**
wavelet	13.4	8.6	5.6	**40.1**	18.0

All the algorithms, except wavelet, performed very well for the measurements obtained in sitting position. Only *ecgpuwave* and *run_sqrs* showed notable errors: FN=1.6% and FP=5.7% respectively. While running, again *run_sqrs* and the wavelet approach had by far lowest performance with FN=46.3% and FP=40.1%, respectively. The *wqrs* showed high FP=21%, whereas *sqrs* had high FN=14.3%. The

This project has received funding from the European Union's Horizon 2020
research and innovation programme under grant agreement No 769661

run_sqrs, *sqrs* and the wavelet approach failed mostly on two noisy measurements obtained while running; in those measurements it was even hard to determine visually the R-peaks correctly. The other methods performed surprisingly well even on those very noisy signals. Considering the overall percentage of the faulty detected peaks, the four best-performing algorithms were *jqrs*, *ecgpuwave*, *gqrs*, and *wqrs* (see Table 2).

3.4. Outcome

To summarize, on twenty measurements obtained from ten people in two different setting, we have shown that most of the examined heartbeat detection algorithms perform very well, even though the signals obtained were not filtered before processing and were quite noisy, which is expected from the ECG obtained while running by using patch ECG device with two electrodes.

4. HEARTBEAT CLASSIFICATION

4.1. Background and Objectives

Unobtrusive wireless ECG measurements obtained by devices employing smaller number of leads provide an opportunity for continuous supervision for the patients with cardiovascular disorders. The main advantage of such “off the person” measurements is obtaining longer and more heterogeneous measurements, meaning the measurements are acquired during different daily activities and, therefore, are more disturbed by noise. Nevertheless, these devices enable real-time tracking of the state of the patient, at the cost of more complicated tasks for automatic detection of specific type of arrhythmia.

The Association for the Advancement of Medical Instrumentation (AAMI) provides a standard to which different methodologies for heartbeat classification are being tested. Similar recommendations are also part of the IEC 60601-2-47 standard. A part of the recommendation is to use the MIT-BIH database for benchmark [23]. The MIT-BIH database is well-established standard database for testing different heartbeat classification methodologies. The database consists of 48 half-hour expert labelled two-channel ambulatory ECG recordings collected from 47 subjects. It includes heartbeats from 5 classes: nonectopic (N), supraventiricular ectopic beat (SVEB), ventricular ectopic beat (VEB), fusion beat (F) and unknown beat (Q). The sub-classes of each class, along with their symbols, are given in Table 3. The N class contains mainly normal heartbeats that dictate normal sinus rhythm. Supraventricular ectopic beats, like atrial premature beats, are a common cardiac arrhythmia characterized by premature

This project has received funding from the European Union's Horizon 2020 research and innovation programme under grant agreement No 769661

heartbeats originating in the atria. Ventricular ectopic beats, like premature ventricular contractions, are extra heartbeats that begin in one of the heart's ventricles. These extra beats disrupt the regular heart rhythm and can be felt as a fluttering or a skipped beat in the chest.

Table 3: Classes (groups) of heartbeats present in the MIT-BIH database.

Class	Symbol	Sub-class
N (Any heartbeat not categorized as SVEB, VEB, F or Q)	N or .	Normal beat
	L	Left bundle branch block beat
	R	Right bundle branch block beat
	e	Atrial escape beat
	j	Nodal (junctional) escape beat
SVEB (Supraventricular ectopic beat)	A	Atrial premature beat
	a	Aberrated atrial premature beat
	J	Nodal (junctional) premature beat
	S	Supraventricular premature beat
VEB (Ventricular ectopic beat)	V	Premature ventricular contraction
	E	Ventricular escape beat
F	F	Fusion of ventricular and normal beat
Q (Unknown beat)	P or /	Paced beat
	f	Fusion of paced and normal beat
	U	Unclassifiable beat

Recent studies overview different sets of features being employed for the task of ECG arrhythmia classification [24, 25]. Most of the studies focus on feature extraction from measurements from at least two leads. However, it was shown that differential ECG leads provide different ECG signals from standard bipolar or unipolar ECG leads [26, 27]. It has been confirmed that the ECG from a differential lead is appropriate for hearth rhythm diagnostics [28]. Traditionally, the problem of heartbeat classification is recognized as a problem of classification of time series. Until recently, the main focus was on the extraction of useful features from time series. However, with the recent advances in the area of deep learning, the focus is shifted towards automatic learning of features from time series [29, 30,

This project has received funding from the European Union's Horizon 2020 research and innovation programme under grant agreement No 769661

31]. Moreover, it has been shown that domain specific time series features might not be informative enough for solving a given time series classification task [32]. Furthermore, time series features derived from other domains showed to be competitive or better than the domain specific features.

Combining global time series features under the AAMI inter-patient paradigm was the main focus in this task. The inter-patient paradigm refers to the process of discarding heartbeats from the same patients in both training and test sets. The final goal is to find features that characterize different classes of heartbeats.

4.2. Material and Methods

In [33], a library for extracting global features from time series data, named HCTSA (Highly Comparative Time Series Analysis), is proposed. The features originate from interdisciplinary studies interested in dynamical modelling. Such global features quantify patterns in time series across the full time interval. The experiments in [33] show that features facilitating interpretable insights are often selected from unexpected literature (drawing attention to novel features for specific application) and best performing classifiers are often constructed using a novel combination of interdisciplinary features (e.g., combining features from economics and bio-medical signal processing). Motivated by these conclusions, we employed this library to the problem of heartbeat classification on a single-lead ECG (MLII) from the MIT-BIH database, following the AAMI recommendations.

The HCTSA library combines time series global feature operators derived across various scientific areas during the years. Roughly, it can be organized into 14 groups: statistical, measures of distribution, correlation, basic function representation, stationary, scaling, entropy, non-linear time series analysis, non-linearity, time domain transformations, model fitting and forecasting, domain specific operators, fanciful operations and others. Each of these groups has its own subgroups of operators. Setting different parameters for operations yields different features. Thus, instead of 1064 basic operations, one can easily finish with few thousand features. Increasing the number of features comes with a cost expressed in time needed for computation and increasing the correlation between the generated features. The later can increase the redundancy in the data and consequently make harder to distinguish the right features for performing the classification task. Regarding the time complexity, calculating features is expensive. However, selecting the right features will result in low cost for obtaining predictions by a pre-trained model. This makes the approach useful in scenario where a fast prediction is needed. The implementation of the library is in MATLAB and is freely available for non-commercial purposes[4].

[4] https://hctsa-users.gitbook.io/hctsa-manual/

This project has received funding from the European Union's Horizon 2020
research and innovation programme under grant agreement No 769661

The 44 records from lead MLII of the MIT-BIH database are first segmented. The cut-off time for the segments is 200 ms before the R peak time – the approximate duration of the PR interval. The segmented heartbeats are given as an input to the HCTSA library and the result is 7873 produced features per heartbeat. Some of the operations showed to be not suited for small number of samples and resulted in errors that are tracked by the library. The processing of the calculated features is performed with removing the features where those errors appeared, which resulted in 3324 total number of features. Since many of the features are a product of one particular operator instantiated with different parameter settings, high correlation between the features could be expected. To assess the relevance of the features, we performed feature ranking using random forests impurity scores [34]. The feature ranking has two goals. First, it provides additional insights into the feature relevance/importance for the classification. Second, it can help in reduction of the number of features used for classification. To select the features, a threshold on the relevance is imposed. In such a way, the features that have higher relevance over the specified threshold are preserved.

The last step in the workflow is using algorithms to build predictive models. As a set of predictive modelling algorithms, AdaBoost and Gradient Boosting, implemented under the scikit-learn library, were used[5]. According to the inter-patient paradigm proposed in [35], the heartbeats from the MIT-BIH database were divided into two sets. The first data set (DS1) is composed of all heartbeats of records: 101, 106, 108, 109, 112, 114, 115, 116, 118, 119, 122, 124, 201, 203, 205, 207, 208, 209, 215, 220, 223 and 230. The second data set (DS2) is composed of all heartbeats of records: 100, 103, 105, 111, 113, 117, 121, 123, 200, 202, 210, 212, 213, 214, 219, 221, 222, 228, 231, 232, 233 and 234. DS1 was used to construct the classification model, while DS2 was reserved for testing. In this way, we guarantee that the created model has no contact with the heartbeats pertaining to DS2, i.e., heartbeats from DS1 and DS2 come from different individuals. The heartbeat distribution by classes of the data sets is given in Table 4.

Table 4: Heartbeat distribution by classes of the train (DS1) and test (DS2) data sets.

Set	N	SVEB	VEB	F	Q	Total
DS1	45866	944	3788	415	8	51021
DS2	44259	1837	3221	388	7	49712
DS1+DS2	90125	2781	7009	803	15	100733

[5] https://scikit-learn.org/stable/

This project has received funding from the European Union's Horizon 2020 research and innovation programme under grant agreement No 769661

According to the AAMI guidelines, we calculate four performance metrics: accuracy, positive predictivity (pp), sensitivity and specificity. Their definitions are as follows:

$$accuracy = \frac{TP + TN}{TP + TN + FP + FN},$$

$$pp = \frac{TP}{TP + FP},$$

$$sensitivity = \frac{TP}{TP + FN},$$

$$specificity = \frac{TN}{TN + FP},$$

where TP, TN, FP and FN are the numbers of true positives, true negatives, false positives and false negatives, respectively.

4.3. Results and Discussion

The time required for computation of all features for 100 733 time series was 240 hours on a single machine with 32GB of RAM and Intel(R) Core(TM) i7-8700K CPU @ 3.70GHz processor. This is a big overhead, but the used post-processing methods aim at reducing the number of features thus reducing the time overhead.

Fig. 6 represents visualization of the training dataset obtained with t-distributed stochastic neighbour embedding (TSNE) from the MIT-BIH database, as discussed in [35]. A clear dealination of the classes can be observed, with the VEB class at the top of the predominantly N class spherical shape and partial localization of SVEB and F classes. Given the spread of the SVEB classes, it can be concluded that algorithms will have hard time in distinguishing the SVEB class from the N class. However, comparing the VEB and the N classes, the separation is clearer.

In Fig. 6, a dozen groups of points are observed. With close inspection of these groups, it can be concluded that they belong to the same patient (Fig. 7). It is important to note that, although the majority of the heartbeats for one patient will happen to belong to one group, there exist heartbeats that do not belong to the same group, if the heartbeats are of different class. For example, beats for the patients 208 and 209, as observed in Fig. 7. This is encouraging finding since it suggests good features for separation of at least some of the classes.

This project has received funding from the European Union's Horizon 2020 research and innovation programme under grant agreement No 769661

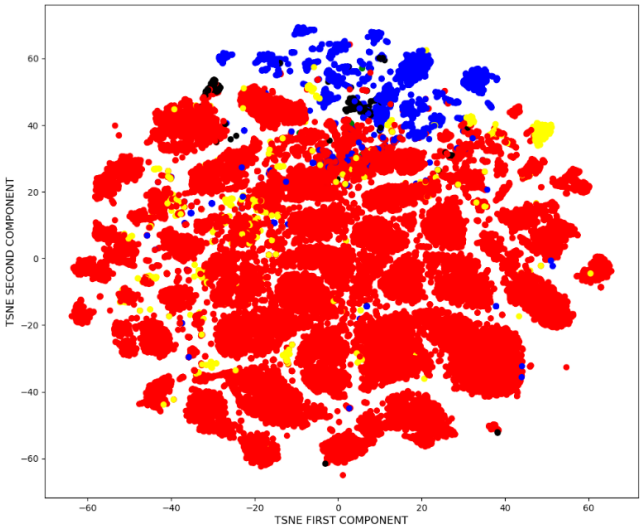

Figure 6: TSNE representation of the training MIT-BIH dataset represented in two dimensions. Classes: N=Red, VEB=Blue, SVEB=Yellow, F=Black, Unknown=Green.

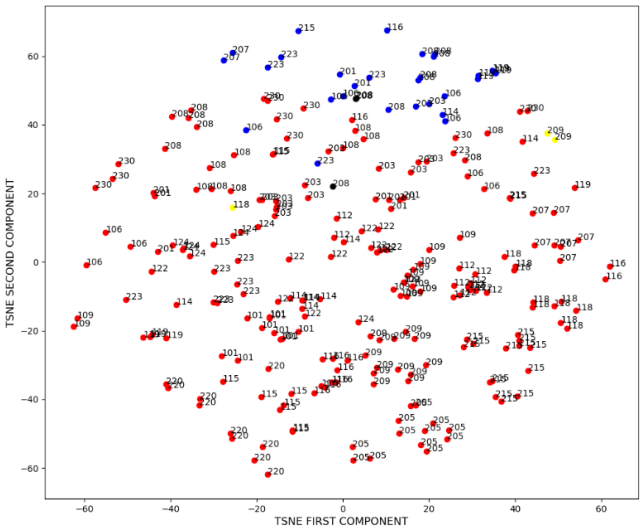

Figure 7: TSNE representation of the training MIT-BIH dataset represented in two dimensions along with patients IDs to present the clustering groups depicted in Fig. 6. Red=N, Blue=VEB, Yellow=SVEB, Black=F, Green=Unknown.

This project has received funding from the European Union's Horizon 2020
research and innovation programme under grant agreement No 769661

The average features rankings with the gini impurity criteria method for all the classes are given in Table 5. From the results presented in Table 5, according to the feature importance for distinguishing a given class from all the rest, it can be conducted that the two most common classes, N and VEB, have features that occur frequently as top ranked. Moreover, the same top ranked features are shared between the N and VEB classes. For example, *Co add noise* – the best ranked feature, comes from the chaos theory. It is a measure of chaos, calculated by adding Gaussian noise to the time series in increasing manner across some range of values and then measuring the mutual information at each point by calculating histograms. The larger the measure, the greater the relative intensity of the chaos is. Predominantly, the values for the N beats tend to be positively valued. According to this measure, positive values indicate chaotic behaviour. Conversely, the VEB heartbeats tend to have negative value for this feature. For both N and VEB, this is the most important feature.

Next, the *normalized length* feature is closely related with one of the most exploited features in heartbeat classification literature – normalized R-R interval. *Normalized length* measures the length of the time series normalized with respect to the average length of the patient-specific heartbeat. Fig. 8 depicts the *normalized length* feature vs. the *CO add noise* feature. It can be seen that the *CO add noise* feature makes separation between classes VEB (blue) and N (red) with observation that VEB heartbeats tend to have larger duration with respect to normal ones. Inspection of the N heartbeats with negative value for the *CO add noise* feature suggests that they belong to patient that experiences VEB heartbeats. Combining this novelty feature together with previously known features enables clearer separation of classes N and VEB. The same discussion for the SVEB and the VEB classes can be drawn in parallel. In Fig. 9, one can also observe a clearer separation of the VEB vs all other classes, which the second ranked feature *CO TranslateShape circle 25 pts fives* imposes. This feature calculates the number of points that are close to certain geometric shapes in plots generated from the time series with lag *t*. As such, those represent measures for point density estimation.

This project has received funding from the European Union's Horizon 2020
research and innovation programme under grant agreement No 769661

Table 5: Top 5 average ranks for the features for the classes N, SVEB, VEB, F and Q.

Vs all	Average rank	Feature name
N	1.7272	CO Add Noise 1 gaussian firstUnder75
	2.2727	CO TranslateShape circle 25 pts fives
	6.5000	EX MovingThreshold 01 01 maxq
	8.4545	EN CID minCE1
	8.5909	SP Summaries pgram hamm w10 90
SVEB	4.6818	CP ML StepDetect l1pwc 005 medianstepint
	4.7727	FC Surprise T2 50 3 udq 500 tstat
	4.9090	PP Compare resample 1 2 gauss1 kd resAC2
	9.31818	CP ML StepDetect l1pwc 02 minstepint
	11.5454	Length
VEB	2.5454	CO AddNoise 1 gaussian firstUnder75
	3.6363	SP Summaries pgram hamm w10 90
	4.5454	EN CID minCE1
	6.5454	CO StickAngles y std p
	7.0454	PH Walker momentum 2 w std
F	15.4545	DN SimpleFit sin1 resruns
	19.9545	CO TranslateShape circle 15 pts threes
	21.0000	PH Walker biasprop 01 05 res runstest
	25.3181	PP Compare spline44 gauss1 kd resruns
	30.1818	HT DistributionTest lillie ev
Q	2.9545	FC LocalSimple mean1 ac1
	3.5454	FC LocalSimple mean3 ac1
	7.0000	MF steps ahead ar 2 6 rmserr 1
	7.6818	FC LocalSimple mean2 ac1
	10.9545	MF AR arcov 2 a3

This project has received funding from the European Union's Horizon 2020 research and innovation programme under grant agreement No 769661

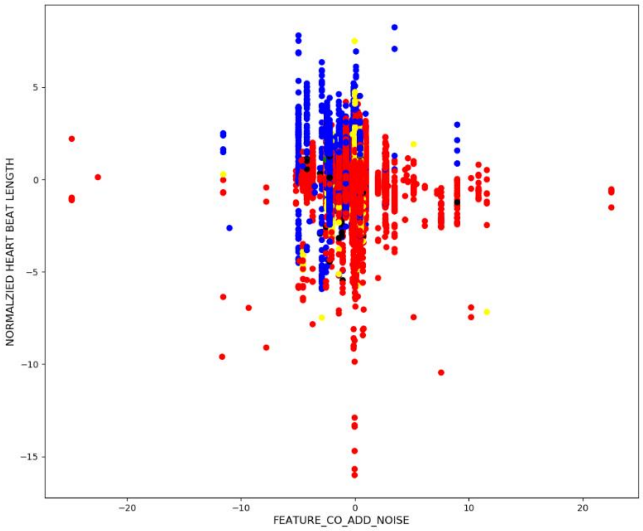

Figure 8: Feature CO add noise – x axis and Feature normalized time series length – y axis. Depicts the separation of VEB versus SVEB and N.

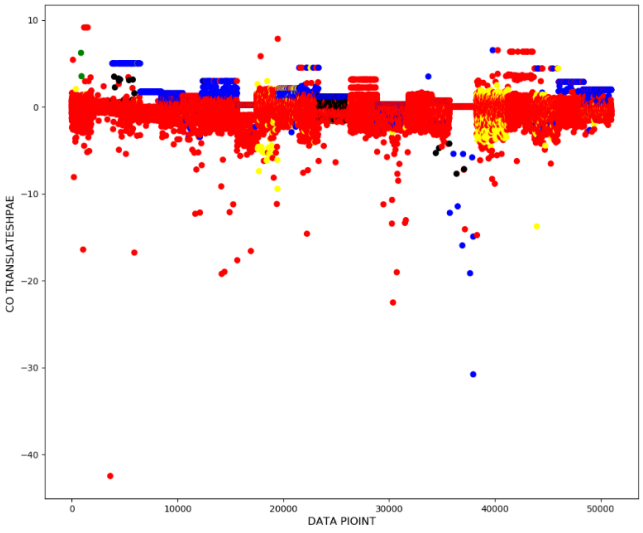

Figure 9: Sample ID – x axis and Feature CO TranslateShape circle 25 pts fives – y axis. Depicts the separation of VEB and N.

This project has received funding from the European Union's Horizon 2020
research and innovation programme under grant agreement No 769661

Regarding the categorization of the SVEB class, such calculated global features do not preserve the local deviation of the SVEB and the N classes. These two types are distinct only in the PR interval of the heartbeat. The global time series features diminish the effect of this local property and thus it is harder to separate the classes N and SVEB. Therefore, a more suitable way would be to threat that part of the heartbeat as separate time series. Extracting features on that part hopefully will bring additional discrimination power.

For class F, the average feature rankings suggest that there is no strong feature for classification of this class. The time series for class Q are varying by large margin in patients, and are of little support. Although, *FC LocalSimple mean1 ac1* appears quite frequently as top ranked feature, its impact cannot be well determined due to overlapping of class distributions by large extent.

The confusion matrix for the best performing AdaBoost model is given in Table 6. It shows that the proposed features are good enough for separation of VEB and other classes. The accuracy, sensitivity, positive predictivity and specificity for the VEB class are: 0.97, 0.76, 0.80 and 0.99 accordingly, which are quite good given the imbalance of the problem. All SVEB heartbeats tend to be predicted as N due to the previously discussed reasons. The accuracy, sensitivity, positive predictivity and specificity for the SVEB class are: 0.96, 0.01, 0.13, and 0.99. The low value for the sensitivity is unsatisfactory. The F and Q beats as expected, are not distinguishable and thus are miss-classified.

Table 6: Confusion matrix for the best performing AdaBoost model. Number of trees: 500, learning rate: 0.1.

	Class	**N**	**SVEB**	**VEB**	**F**	**Q**
True label	**N**	43832	25	396	3	0
	SVEB	1721	15	100	1	0
	VEB	708	76	2432	4	0
	F	281	1	106	0	0
	Q	3	0	0	4	0

Compared to the state-of-the-art methods that extract features from a single-lead ECG, our approach has lower classification performance. One of the explanations, as also presented in the work performed in [31], is that extracting patient specific features can help in solving the task. As depicted in Fig. 6, the

This project has received funding from the European Union's Horizon 2020 research and innovation programme under grant agreement No 769661

heartbeats of same patient tend to cluster themselves in groups. This might reflect the belief of unique anatomy of a patients' cardiovascular system, which implies different characteristic features of the types of arrhythmia a patient might experience. Also, in their work, information for the neighbouring heartbeat is used, which seems useful, since the heartbeats are not independent.

4.4. Outcome

To conclude, we propose methods for feature extraction in single-lead ECG for the purpose of heartbeat classification. The extracted features belong to the domain of global time series features derived from various technical and scientific areas. Results show that features that emerge from different scientific areas can provide information for separation of different class distributions that appear in the heartbeat classification problem. The extracted features are discriminative for the VEB class versus the remaining 4 classes. However, a clear distinction between non-ectopic and SVEB heartbeats is absent. This is due to the focus of the employed time series features to extract the global properties – non-ectopic and SVEB heartbeats are different mostly in the PR interval. Thus such global approach might not be suitable. In future, we would test if building patient specific models for heartbeat classification improves the predictive performance.

5. ENRICHING ECG WITH ACTIVITY DATA

5.1. Background and Objectives

The information on the user's daily activities has been already recognized as significant extension to ECG measurements. For that purpose, the Holter users need to write down the information on their daily activities regularly. In practice, this information usually ends up faulty with lots of activity events missing or misaligned in time with collected ECG data. Such information leads to an increased medical technician time for data cleaning, an increased physician time for making a diagnosis and an increased error rate in diagnosis. In previous studies, an approach to overcome these problems was an automatic augmentation of ECG data with data collected from an accelerometer sensor. Combining accelerometer with the ECG data enables additional insights into patient current activity state. Several prototypes of a system which fuses the ECG data with accelerometer data to monitor the current physical state of the user in wellness facilities have been presented in [36] and [37]. An adaptive reduction of artefacts caused by electrode-skin impedance change during motion was described in [38]. Additionally,

This project has received funding from the European Union's Horizon 2020 research and innovation programme under grant agreement No 769661

accelerometer data were used to detect specific user's physical settings or the context, as presented in [39]. Context detection was presented for health and ECG monitoring applications in [40] and [41].

In the present feasibility study, we propose and evaluate a simple method for fusing ECG and accelerometer data streams with the aim to improve ECG interpretation accuracy regarding disturbing noise, e.g. electrode movements, muscular activity, etc. For example, if a user is in a lying position and not active, her/his heart rate could not be higher than 80 beats/s, or, if the user is highly active, her/his beat rate is expected to be between 80 and 180 beats/s. However, the results from the heartbeat detector could be interpreted now with higher fidelity even that the interpretation results are based on a potentially more disturbed ECG signal.

5.2. Measurement Procedure

Experimental measurements of ECG and activity data have been obtained by two highly sensitive sensors: the Savvy wireless ECG body sensor and a motion sensor. The measurements were obtained from a single subject who give an informed consent to use the acquired data for research purposes. The motion data have been obtained from a separate custom prototype motion sensor based on Arduino Due[6] for controlling MPU9250 devices[7]. The MPU9250 is a two-chip Micro Electro Mechanical System (MEMS) with both chips packed into a single package. The first chip is a highly sensitive 3-axis gyroscope and 3-axis accelerometer, both with 16 bits A/D converters and sample rates of up to 8000 samples/s. The second chip is a 3-axis electronic compass based on a highly sensitive Hall sensor technology AK8963 with selectable 14/16 bits A/D converters and sample rates up to 100 samples/s. The motion data analysis was performed in our case with the 3-axis accelerometer only. Data acquisition and moving window filtering was performed by a custom Arduino firmware. The measured data were passed to an output communication port and saved as a log file in textual format. Note that the accelerometer module is already incorporated in the Savvy sensor in order to be activated by sensor firmware after the presented feasibility study is finished.

The ECG and motion sensors have been fixed in the proximity of the heart on the frontal side of the thorax as shown in Fig. 10. The Savvy sensor was fixed with standard ECG electrodes while the motion sensor was fixed with self-adhesive tape. In order to time align both received data streams, a clearly detectable event on both sensors was required. For that purpose, we used a few hand taps on both sensors before starting the measurements. The sample rate of ECG was 128 samples/s while each of 3-axis of motion data was sampled by 100 samples/s. The ECG and motion data have been measured for

[6] https://www.arduino.cc
[7] https://www.invensense.com/products/motion- tracking/9axis/mpu-9250/

This project has received funding from the European Union's Horizon 2020 research and innovation programme under grant agreement No 769661

approximately 18 minutes in a continuous measurement separated into 11 steps under the protocol shown in Table 7. The transitions between the phases typically lasted about 15 seconds. The transition time was part of the duration time for each phase of the measurement.

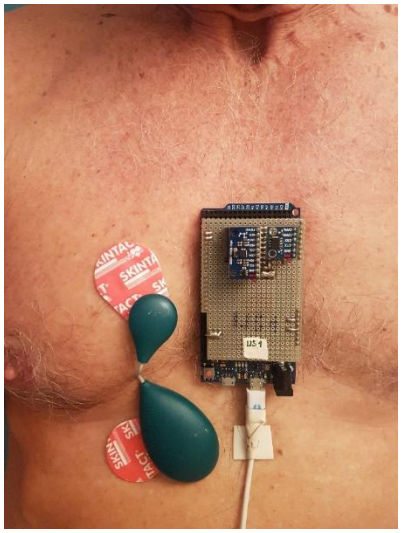

Figure 10: ECG and motion sensors fixed on the frontal side of the thorax.

Table 7: Measurement phases.

Phase	Activity	Pose	Duration [min]
1	lying	pre-measurement resting	2
2	activation of both sensors	5 hand-taps on both sensors	0.25 - start of measurements
3	resting	laying on back	2
4	resting	laying on right arm	2
5	resting	laying on stomach	2
6	resting	laying on left arm	2
7	resting	sitting	2
8	resting	staying upright	2
9	walking	staying upright	2
10	running	staying upright	2
11	deactivation of both sensors	5 hand-taps on both sensors	0.25 - end of measurement

This project has received funding from the European Union's Horizon 2020 research and innovation programme under grant agreement No 769661

Raw signals for the accelerometers, in each dimension, and the ECG are shown in Fig. 11. Because we used two separate sensors, a time alignment was performed by comparing the effect of simultaneous hand-taps on both sensors. In our case, shown in Fig. 11, a shift of +1876 ms was applied on all three acceleration data channels. The raw acceleration data contain an initial constant error of the device. This error is called bias, and it differs for each sensor unit. To gain more accurate results, the raw accelerometer data were corrected by subtracting the bias values. In our case, the accelerometer sensor has bias values equal to: Xbias = 0.095094 ms^{-2}, Ybias = 0.0389 ms^{-2}, Zbias = -1.3567 ms^{-2}. Bias value for each axis can be acquired by measuring acceleration values when the axis is placed vertically to the gravity in both directions, positive and negative. The bias is then computed as an average between these two values.

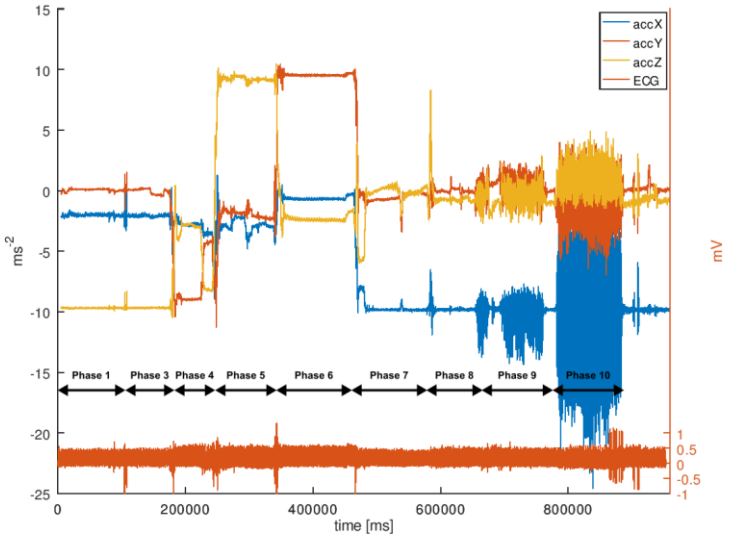

Figure 11: ECG and acceleration measurements aligned in time.

5.3. Analysis

The acquired accelerometer data were used for estimating body pose of a person using the device. For this purpose, we defined six different poses to be determined:

- Pose 0 – undefined pose,
- Pose 1 – laying on back,
- Pose 2 – laying on right arm,
- Pose 3 – laying on front,
- Pose 4 – laying on left arm,
- Pose 5 – straight up.

This project has received funding from the European Union's Horizon 2020
research and innovation programme under grant agreement No 769661

The pose was estimated through the two-step process. First, all of the acceleration data were filtered with second-order Butterworth low-pass filter with cut-off frequency at 0.2 Hz. The primary purpose of this step is to remove the high-frequency activity component from raw data. Filter cut-off value of 0.2 Hz was chosen as the best trade-off between time delay and noise reduction. The values were obtained by running a series of benchmark tests with the second-order low-pass filter. This step is not essential. However, it ensures better quality and robustness of end pose estimation results. The second step is rule-based estimation with a threshold equal to 4.905 ms^{-2}, which is half of the gravity acceleration. Taking into account the gravity acceleration is time-invariant, the vector sum of all axes value must be equal to the gravity acceleration. If a single axis gains value greater than half of the gravity acceleration, then two other axes must have lower values. Therefore, the first axis is the dominant one. Intermediate and final results of the pose estimation are shown in Fig. 12.

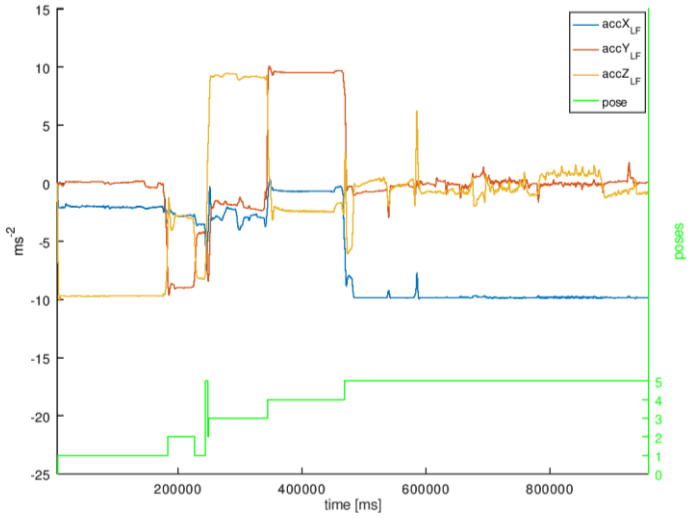

Figure 12: Filtered acceleration data and pose estimation.

Similarly, the activity indicator was also determined through the two-step process. Activity is not related to poses and it simply measures the average acceleration. In this case, we extracted high-frequency activity component from raw data by filtering each channel of acceleration data with second-order Butterworth high-pass filter with cut-off frequency at 0.5 Hz. As in the low-pass filter for pose estimation, the cut-off of 0.5 Hz showed to be the best value to separate low-frequency pose information from high-frequency activity information. After applying the filter, absolute values of

This project has received funding from the European Union's Horizon 2020
research and innovation programme under grant agreement No 769661

filtered data were averaged with moving-average with 100 samples wide window. The end activity result is a sum of the X, Y and Z axes values. All results of the activity determination process are shown in Fig. 13. Activity values represent the magnitude of change in acceleration, and thus can also be expressed in ms^{-2} units.

After we have extracted pose and activity information from the accelerometer data, we have combined it with the ECG signal. In Fig. 14, we can see that the transition between poses (yellow line) raises physical activity (red line), which influences the ECG signal. For the case in the figure, we can conclude that artefact in ECG signal is triggered by an external cause (e.g. change in body pose) and not internally (e.g. heart disease).

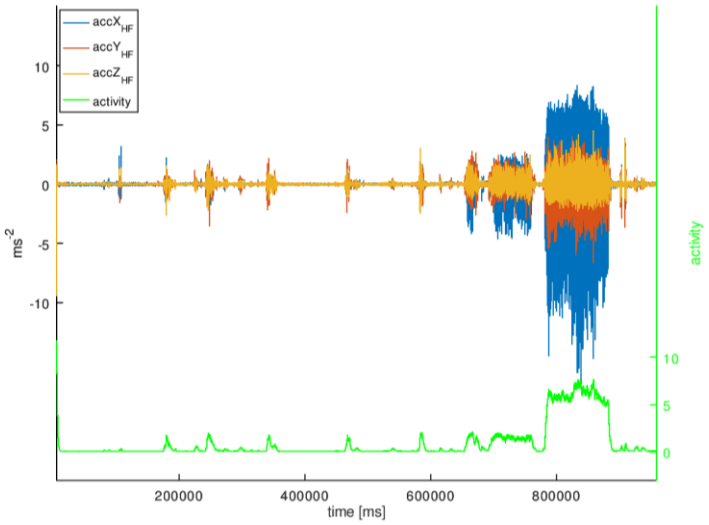

Figure 13: Filtered acceleration data and activity.

This project has received funding from the European Union's Horizon 2020
research and innovation programme under grant agreement No 769661

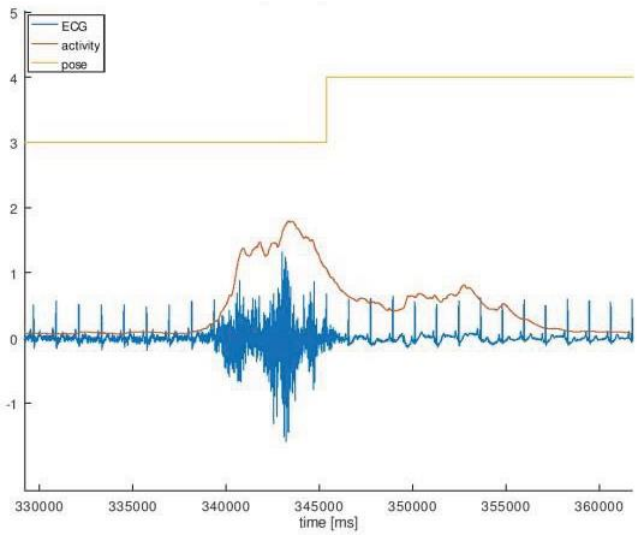

Figure 14: A zoomed interval of pared ECG signal with activity and pose information during transition between phases 5 and 6 (transition from pose 3 to pose 4).

5.4. Calculation complexity

From the practical and economical point of view, the upgraded ECG device should perform the necessary data processing and analysis either on the existing microprocessor inside the ECG sensor or on a smartphone device that communicates with the ECG sensor. In both cases, computing, memory and communication resources are limited, and thus all of the processing needs to be simplified to minimise the count of operations. The resource limitations are the main reason to use second-order Butterworth filter, which requires for each filtered value only 5 multiplications and 4 additions/subtractions between two float values:

$$F_n = b_0X_n + b_1X_{n-1} + b_2F_{n-2} - a_1F_{n-1} - a_2F_{n-2}.$$

The original 100-samples wide moving-average window requires minimally 4 operations (2 multiplications and 2 additions/subtractions), and the last 100 samples and the mean value of the previous sample have to be stored. To additionally reduce calculation and memory complexity, we replaced the moving-average with an exponential moving-average (EMA) that can be calculated by a simple equation:

$$EMA(t) = \begin{cases} X(t), & t = 1 \\ \alpha X(t) - (1-\alpha) * EMA(t-1), & t > 1 \end{cases}.$$

This project has received funding from the European Union's Horizon 2020
research and innovation programme under grant agreement No 769661

In this case, we use α equal to 0.01 to represent values similar to the moving-average with 100-samples wide window. If we use a buffer to store 3 values (α, $1-\alpha$, and EMA of the previous sample), the calculation includes only 2 multiplications and 1 addition between two float values. As shown in Fig. 15, for this case, the difference between moving-average and EMA is negligible.

5.5. Outcome

To summarize, we have conducted a feasibility study aiming at enriching ECG data collected from Savyy ECG body sensor with pose and activity information. Activity and pose estimation were extracted from data collected with the accelerometer device fixed to the user's frontal side of the thorax. The obtained experimental results show a high correlation between actual and estimated pose and activity. The results provide an additional real-time context of the user condition to make ECG data more interpretable. Furthermore, we built a model to calculate pose and activity estimation that exhibits a very low number of simple mathematical operations. Such a model is suitable for devices with limited processing power such as extremely low power signal processors, or low power radio communication with smartphones or similar personal devices.

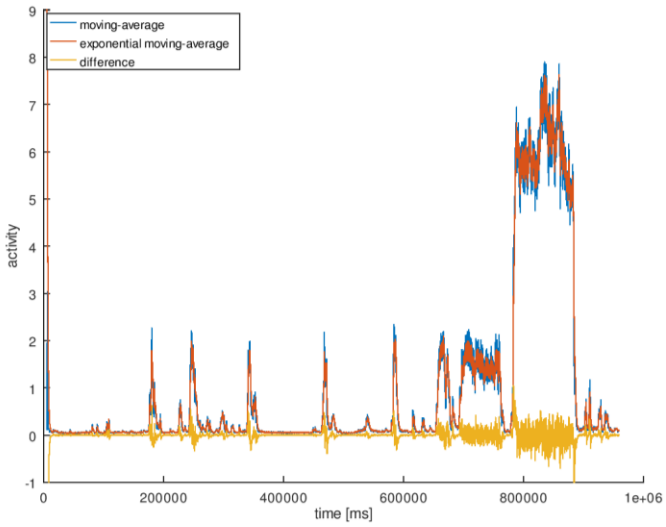

Figure 15: Activity moving-average and exponential moving-average comparison.

This project has received funding from the European Union's Horizon 2020
research and innovation programme under grant agreement No 769661

6. INTEGRATION OF THE CARDIO-VASCULAR MODULE IN THE SAAM INFRASTRUCTURE

In this section, we describe the procedures and the activities conducted for integration of the cardio-vascular devices and services into the SAAM infrastructure. First, we present the connection procedures of the devices, i.e. the Savvy ECG sensor and the blood pressure monitor, to the SAAM platform. According to the SAAM system architecture described in D1.8, the first contact point of the SAAM system to these devices is the Edge GW. After that, we describe the feature extraction from the ECG signal on the Edge GW. These features will be further processed in the SAAM system. At the end, we present two scenarios for piloting and testing the cardio-vascular module in the SAAM system.

6.1. Connecting the Cardio-vascular Devices into the SAAM Architecture

In order to connect the Savvy ECG device to the Edge GW, we have implemented the PCARD Wireless Protocol (PWP) on the Edge GW via BlueZ Linux drivers and a higher level Python library. This implementation allows for streaming ECG measurements to the Edge GW without the need for external hardware.

We have tested the Edge GW Bluetooth capabilities. The Edge GW is a stationary device, with a limited BLE range. With ideal positioning of the Edge GW, full BLE coverage of an apartment is sometimes possible, but lost packets are to be expected.

Received raw ECG on the Edge GW can be stored, transmitted or used for ECG feature extraction. Retrieved information can be transmitted directly to the SAAM database via MQTT protocol. The unit tests conducted in laboratory setting (running Python software on PC and Edge GW) include: (i) transmission of ECG signal from the Savvy sensor to the Edge GW and time alignment, (ii) transmitting data via MQTT from the Edge GW to the SAAM database.

For the BPM device, a standard BLE service is used to communicate to the BPM and transfer the measurements to the Edge GW. We implemented a python wrapper that allows an application on the Edge GW to auto-connect to the BPM and download measurements from it without user's intervention. In case a user measured their blood pressure outside of the BLE range, the BPM holds history of the 9 last measurements taken. On each connection established with the Edge GW, all 9 measurements are transmitted, minimising the chance of lost measurements. The Edge GW is constantly scanning for the BPM device, and after a BPM measurement is done, it can be transmitted to the SAAM database via MQTT. The unit tests conducted include: (i) receiving and parsing blood pressure measurements via BLE

This project has received funding from the European Union's Horizon 2020 research and innovation programme under grant agreement No 769661

from the BPM to the Edge GW, (ii) transmitting data via MQTT from the Edge GW to the SAAM database.

6.2. ECG Feature Extraction

For the tasks of modelling, profiling and coaching in WP4, we provide heart-related features extracted from the raw ECG signal. The extraction of features is performed on the Edge GW. This means that the raw ECG data is transferred from the Savvy sensor to the Edge GW only. As our previous studies have shown, a feature that can be reliably extracted from a patch ECG reading is the R peak time. i.e. the heartbeat detection. Having the R-peak time, we can easily calculate the heart rate (HR) as a more common feature. As we are interested in real-time heartbeat detection, we have selected the Pan-Tompkins algorithm for QRS detection to be used in the SAAM implementation. According to the results from the study presented in Section II, the Pan-Tompkins algorithm has showed very satisfactory results in heartbeat detection, even in ECG measurements acquired during intense physical activity, like running. Moreover, having in mind that the feature extraction should not have high computing power requirements, since the Edge GW has limited computing capacity, the Pan-Tompkins algorithm is the right choice because it was designed for real-time QRS detection and does not require excessive computing power.

The Pan-Tompkins algorithm reliably recognizes QRS complexes based upon digital analyses of slope, amplitude, and width [20]. A special digital band pass filter reduces false detections caused by the various types of interference present in ECG signals. Furthermore, this filtering permits use of low amplitude thresholds in order to get high detection sensitivity. The algorithm includes dual-thresholds technique and search back for missed beats. Moreover, it periodically adapts each threshold and RR interval limit automatically. This adaptive approach provides good accuracy on diverse ECG signals, QRS morphologies, and heart rate changes. For the standard 24-h MIT-BIH arrhythmia database, this algorithm correctly detects 99.3 % of the QRS complexes.

To port the feature extraction on the Edge GW platform, we have implemented the Pan-Tompkins algorithm in Python. The Python program can easily communicate with the above-mentioned Python library that implements PWP, enabling the measurements to be streamed to the Edge GW and processed there in real time. Due to loose transmission and BLE delays, basic time alignment is done before running feature extraction on the signal. The unit tests conducted include: (i) running the Pan-Tompkins algorithm on the ECG signal on the Edge GW, (ii) transmitting the extracted feature data via MQTT from the Edge GW to the SAAM database.

This project has received funding from the European Union's Horizon 2020
research and innovation programme under grant agreement No 769661

6.3. Testing Scenarios

The Savvy ECG device can be used in SAAM in two possible scenarios. The first one is to integrate it as a part of the SAAM architecture (as described in the SAAM system architecture in D1.8), i.e., transferring the ECG measurements from the user to the Edge GW and extracting ECG relevant features in place, which are further processed in the SAAM system for the purposes of monitoring, modelling and profiling. However, another possible scenario is the ECG sensor to be used as a part of a system for Personal CARDiac (PCARD) monitoring, as suggested in [42]. The proposed PCARD platform is schematically shown in Fig. 16. It starts with measurement of the ECG that incorporates significant information about the personal health state. It then continues with the display of the ECG signal and its analysis on a personal portable terminal (PPT), such as a Smartphone, and on a Cloud-based storage, processing, and visualization software. In this integrated care solution, the ECG measured and processed data are available to the patient as well as to the medical personnel. The personal terminal connects to the ECG sensor via Bluetooth Smart protocol and records everything that the ECG sensor measures. This protocol offers sufficient bandwidth, data encryption and is low power, so it conserves well the batteries of the ECG sensor and the PPT. Power consumption is one of the main limiting factors for device autonomy.

A mobile Android application (MobECG[8]) is installed on the PPT, with main functionalities including: establishing communication between the Savvy sensor and the PPT, visualization of the on-going measurement, storing the measured data on the PPT storage, interaction with the user, and transferring the measurements to a secure storage server or Cloud platform. Furthermore, the MobECG program has an option to generate a summary report of an ECG measurement around a user's marked event. The ECG report is saved in a pdf file and can be shared with a trusted caregiver or a medical expert. The report provides a detailed ECG around a user-marked event during the measurement, e.g., when an activity was initiated or when an inconvenience has been felt. The ECG report is not intended for diagnostic purposes, but for an indication of potential hearth rhythm disturbances. It is of particular value during long-term measurements (from a few days to a month), which are a viable option for screening of hearth rhythm in a larger population.

Four pilot studies have already confirmed the usability of the PCARD system: (1) postoperative atrial fibrillation recognition at the University Medical Center Ljubljana; (2) palpitation detection at the Community Health Centre Ljubljana; (3) short or long term health assessment at the spa and medical centre Terme Dobrna; and (4) short or long term heart condition assessment at the Muscular Dystrophy Association (MDS) rehabilitation center Izola. Furthermore, the PCARD platform has also been used in

[8] https://play.google.com/store/apps/details?id=si.ijs.e6.MobEcg

This project has received funding from the European Union's Horizon 2020 research and innovation programme under grant agreement No 769661

demonstration pilots in the project EkoSmart ("Ecosystem of a Smart City") co-financed by the Ministry of Education, Science and Sport of the Republic of Slovenia through the European Regional Development fund. The pilot studies of cardiac activity included screening of patients on primary level at the Community Health Centre, Ljubljana (30 doctors, 200 patients) and monitoring of atrial fibrillation after surgery at the University Medical Centre Ljubljana (4 doctors, 150 - 200 patients).

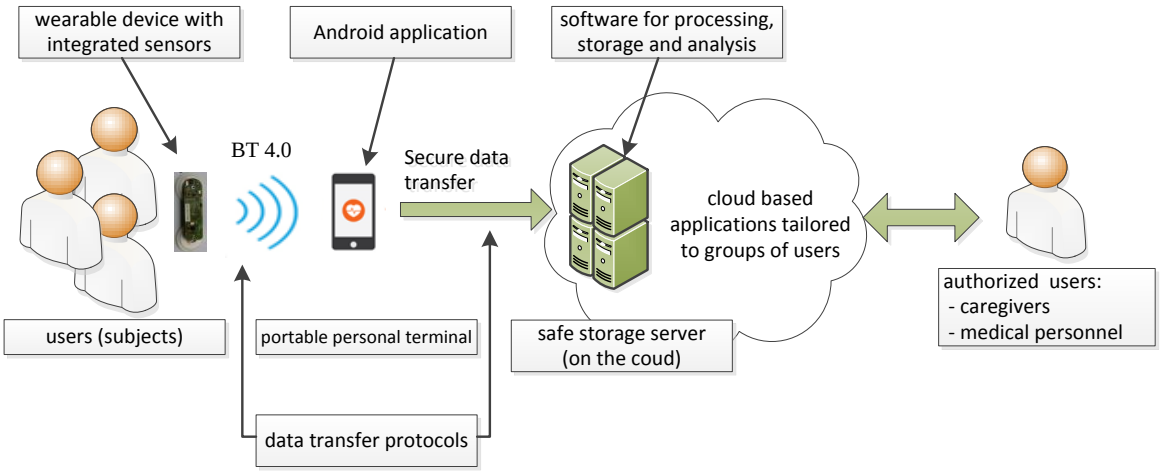

Figure 16: PCARD technology platform for follow-up of cardiac patients.

7. CONCLUSIONS

In this deliverable, concerning the cardio-vascular health monitoring in the SAAM project, we have presented the results of three major research activities: heartbeat detection, heartbeat classification, and fusion of ECG and activity data. In all activities, the Savvy ECG device has been used. The Savvy ECG and a blood pressure monitor are the main cardio-vascular devices integrated into the SAAM infrastructure.

For of heartbeat detection, eight ECG beat detection algorithms were tested on twenty measurement traces, obtained by the Savvy patch ECG device, for their accuracy in heartbeat detection. On each subject, one measurement trace was obtained while sitting and one while running. Each measurement trace lasted from thirty seconds to one minute. The measurement traces obtained while running were

This project has received funding from the European Union's Horizon 2020
research and innovation programme under grant agreement No 769661

more challenging for all the algorithms, as most of them almost perfectly detected all the heartbeats on the measurements obtained in sitting position. However, when applied on the measurement traces obtained while running, all the algorithms have performed with decreased accuracy.

Next, we have investigated methods for feature extraction in single-lead ECG for the purpose of heartbeat classification. The used feature extraction methods originate from the field of time series analysis. The obtained features are then coupled with a classification algorithm to obtain predictive models. The usefulness of the proposed approach was demonstrated on the MIT-BIH arrhythmia database. Results show that features that emerge from different scientific areas can provide information for separation of different class distributions that appear in heartbeat classification problem.

Furthermore, we have proposed an enhancement of the ECG signal from a wearable ECG device with accelerometer data. The conducted feasibility study aimed to extract and recognize a patient's pose and activity from the accelerometer data. Then, the time-aligned ECG and accelerometer data were fused in order to add valuable information for the interpretation program. In such way, a physician or an interpretation program have further insight into whether the change in heart rate is caused by the irregular heartbeats or by the patient's movement activity. We have validated the proposed methodology on real measurements with ECG and accelerometer data.

Last, but not least, we have presented the activities performed for integrating the cardio-vascular devices into the SAAM system. This includes connecting the Savvy ECG and a blood pressure monitor into the SAAM infrastructure, namely, the Edge GW, and providing services, like real-time ECG feature extraction. Additionally, we have presented the option to use the Savvy ECG in another scenario, i.e. as a part of a system for Personal CARDiac (PCARD) monitoring. In this integrated care scenario, all ECG measured and processed data are available to the patient as well as to the pre-authorized medical and/or caregiving personnel. All these activities have been conducted to support a cardio-vascular pilot study in SAAM.

This project has received funding from the European Union's Horizon 2020
research and innovation programme under grant agreement No 769661

REFERENCES

[1] I. Tomasic, N. Petrovic, M. Lindén, and A. Rashkovska, “Comparison of publicly available beat detection algorithms performances on the ECGs obtained by a patch ECG device,” Proceeding of MIPRO 2019, 42nd International Convention on Information and Communication Technology, pp. 294–297, 2019.

[2] J. Bogatinovski, D. Kocev, and A. Rashkovska, “Feature Extraction for Heartbeat Classification in Single-Lead ECG,” Proceeding of MIPRO 2019, 42nd International Convention on Information and Communication Technology, pp. 339–343, 2019.

[3] I. Grubišić, D. Davidović, B. Medved Rogina, M. Depolli, M. Mohorčič, and R. Trobec, “Enriching Heart Monitoring with Accelerometer Data,” Proceeding of MIPRO 2019, 42nd International Convention on Information and Communication Technology, pp. 328–332, 2019.

[4] R. Trobec, I. Tomasic, A. Rashkovska, M. Depolli, and V. Avbelj, “From multichannel ECG to wireless body sensors,” in Body Sensors and Electrocardiography, Springer International Publishing, 2018, pp. 13–33.

[5] A. Rashkovska, D. Kocev, and R. Trobec, “Clustering of heartbeats from ECG recordings obtained with wireless body sensors,” Proceeding of MIPRO 2016, 39th International Convention on Information and Communication Technology, pp. 461–466, 2016.

[6] S. S. Lovric et al., “Sympathetic reinnervation after heart transplantation, assessed by iodine-123 metaiodobenzylguanidine imaging, and heart rate variability,” Eur. J. Cardio-thoracic Surg., vol. 26, no. 4, pp. 736–741, 2004.

[7] S. Frljak, V. Avbelj, R. Trobec, B. Meglic, T. Ujiie, and B. Gersak, “Beat-to-beat QT interval variability before and after cardiac surgery,” Comput. Biol. Med., vol. 33, no. 3, pp. 267–276, May 2003.

[8] V. Avbelj and R. Trobec, “A closer look at electrocardiographic P waves before and during spontaneous cardioinhibitory syncope,” Int. J. Cardiol., vol. 166, no. 3, pp. e59–e61, 2013.

[9] A. Rashkovska and V. Avbelj, “Abdominal fetal ECG measured with differential ECG sensor,” Proceeding of MIPRO 2017, 40th International Convention on Information and Communication Technology, pp. 289–291, 2017.

[10] M. Jan and R. Trobec, “Long-term follow-up case study of atrial fibrillation after treatment,” Proceeding of MIPRO 2017, 40th International Convention on Information and Communication Technology, pp. 297–302, 2017.

[11] F. Liu et al., “Performance Analysis of Ten Common QRS Detectors on Different ECG Application Cases,” J. Healthc. Eng., vol. 2018, no. 2, pp. 1–8, 2018. doi: 10.1155/2018/9050812.

This project has received funding from the European Union's Horizon 2020 research and innovation programme under grant agreement No 769661

[12] M. Elgendi, B. Eskofier, S. Dokos, and D. Abbott, “Revisiting QRS detection methodologies for portable, wearable, battery-operated, and wireless ECG systems,” PLoS One, vol. 9, no. 1, 2014. doi: 10.1371/journal.pone.0084018.

[13] R. Trobec, I. Tomasic, A. Rashkovska, M. Depolli, and V. Avbelj, “Commercial ECG systems,” in Body Sensors and Electrocardiography, Springer International Publishing, 2018, pp. 101–114.

[14] A. L. Goldberger et al., “PhysioBank, PhysioToolkit, and PhysioNet: components of a new research resource for complex physiologic signals.,” Circulation, vol. 101, no. 23, pp. E215-220, 2000.

[15] I. Silva and G. B. Moody, “An Open-source Toolbox for Analysing and Processing PhysioNet Databases in MATLAB and Octave,” J. Open Res. Softw., vol. 2, no. 1, pp. 1–4, 2014.

[16] A. N. Vest et al., “An open source benchmarked toolbox for cardiovascular waveform and interval analysis,” Physiol. Meas., vol. 39, no. 10, 2018. doi: 10.1088/1361-6579/aae021.

[17] I. Tomasic, V. Avbelj, and R. Trobec, “Smart wireless sensor for physiological monitoring,” in Studies in Health Technology and Informatics, 2015, vol. 211, pp. 295–301.

[18] A. E. W. Johnson, J. Behar, F. Andreotti, G. D. Clifford, and J. Oster, “R-Peak Estimation using Multimodal Lead Switching,” in Computing in Cardiology, 2014, pp. 281–284.

[19] J. Behar, A. Johnson, G. D. Clifford, and J. Oster, “A comparison of single channel fetal ecg extraction methods,” Ann. Biomed. Eng., vol. 42, no. 6, pp. 1340–1353, 2014.

[20] J. Pan and W. J. Tompkins, “A real-time QRS detection algorithm.,” IEEE Trans. Biomed. Eng., vol. 32, no. 3, pp. 230–236, Mar. 1985.

[21] W. Zong, G. B. Moody, and D. Jiang, “A robust open-source algorithm to detect onset and duration of QRS complexes,” Comput. Cardiol., vol. 30, pp. 737–740, 2003.

[22] ©The MathWorks Inc., “R Wave Detection in the ECG,” 2019. [Online]. Available: https://se.mathworks.com/help/wavelet/ug/r-wave-detection-in-the-ecg.html.

[23] G. Moody and R. Mark, “The impact of the mit-bih arrhythmia database,” IEEE Engineering in Medicine and Biology Magazine, vol. 20, no. 3, pp. 45–50, 2001.

[24] S. K. Berkaya, A. K. Uysal, E. S. Gunal, S. Ergin, S. Gunal, and M. B. Gulmezoglu, “A survey on ecg analysis,” Biomedical Signal Processing and Control, vol. 43, pp. 216–235, 2018.

[25] E. J. da S. Luz, W. R. Schwartz, G. Camara-Chavez, and D. Menotti, “Ecg-based heartbeat classification for arrhythmia detection: A survey,” Computer Methods and Programs in Biomedicine, vol. 127, pp. 144–164, 2016.

[26] I. Tomašić and R. Trobec, “Electrocardiographic systems with reduced numbers of leads—synthesis of the 12-lead ecg,” IEEE reviews in biomedical engineering, vol. 7, pp. 126–142, 2013.

This project has received funding from the European Union's Horizon 2020 research and innovation programme under grant agreement No 769661

[27] R. Trobec, I. Tomašić, A. Rashkovska, M. Depolli, and V. Avbelj, Body Sensors and Electrocardiography. Springer International Publishing, 2018.

[28] I. Tomašić, S. Frljak, and R. Trobec, "Estimating the universal positions of wireless body electrodes for measuring cardiac electrical activity," IEEE Transactions on Biomedical Engineering, vol. 60, no. 12, pp. 3368–3374, 2013.

[29] U. R. Acharya, H. Fujita, O. S. Lih, Y. Hagiwara, J. H. Tan, and M. Adam, "Automated detection of arrhythmias using different inter-vals of tachycardia ecg segments with convolutional neural network," Information Sciences, vol. 405, pp. 81–90, 2017.

[30] S. Kiranyaz, T. Ince, and M. Gabbouj, "Real-time patient-specific ecg classification by 1-d convolutional neural networks," IEEE Transactions on Biomedical Engineering, vol. 63, no. 3, pp. 664–675, 2016.

[31] A. Sellami and H. Hwang, "A robust deep convolutional neural network with batch-weighted loss for heartbeat classification," Expert Systems with Applications, vol. 122, pp. 75–84, 2019.

[32] G. Dong and H. Liu, Feature Engineering for Machine Learning and Data Analytics, 2018.

[33] B. D. Fulcher and N. S. Jones, "Highly comparative feature-based time-series classification," IEEE Transactions on Knowledge and Data Engineering, vol. 26, pp. 3026–3037, 2014.

[34] R. Dıaz-Uriarte and S. Alvarez de Andres, "Gene selection and classi-fication of microarray data using random forest," BMC Bioinformatics, vol. 7, 2006. doi: 10.1186/1471-2105-7-3.

[35] P. de Chazal, M. O'Dwyer, and R. B. Reilly, "Automatic classification of heartbeats using ecg morphology and heartbeat interval features," IEEE Transactions on Biomedical Engineering, vol. 51, no. 7, pp. 1196–1206, 2004.

[36] J. Healey and B. Logan, "Wearable wellness monitoring using ECG and accelerometer data," 9th IEEE International Symposium on Wearable Computers (ISWC'05), Osaka, 2005, pp. 220–221.

[37] W. Y. Chung, S. Bhardwaj, A. Punvar, D. S. Lee, R. Myllylae, "A Fusion Health Monitoring Using ECG and Accelerometer sensors for Elderly Persons at Home," 29th Annual International Conference of the IEEE Engineering in Medicine and Biology Society, pp. 3818–3821, 2007.

[38] S. W. Yoon, S. D. Min, Y. H. Yun, S. Lee, and M. Lee, "Adaptive Motion Artifacts Reduction Using 3-axis Accelerometer in Etextile ECG Measurement System," Journal of Medical Systems, vol. 32, pp. 101–106, 2008.

[39] D. Figo, P. C. Diniz, D. R. Ferreira and J. M. Cardoso, "Preprocessing techniques for context recognition from accelerometer data," Personal and Ubiquitous Computing, vol. 14, pp. 645–662, 2010.

[40] P. D. Haghighi, A. Perera, M. Indrawan and T. M. Huynh, "Situation-aware mobile health monitoring," MobiQuitous, 2014.

This project has received funding from the European Union's Horizon 2020 research and innovation programme under grant agreement No 769661

[41] J. P. Li, A Mobile ECG Monitoring System with Context Collection, 2017.

[42] M. Depolli, V. Avbelj, R. Trobec, J. M. Kališnik, T. Korošec, A. P. Susič, U. Stanič, A. Semeja, “PCARD Platform for mHealth Monitoring,” Informatica, vol. 40, 117–123, 2016.

This project has received funding from the European Union's Horizon 2020
research and innovation programme under grant agreement No 769661